NIPPON STEEL TECHNICAL REPORT No. 123 MARCH 2020

Technical Report

UDC 662 . 741

Imaging Diagnosis Technology for Coking Chamber Walls

Masato SUGIURA* Yoshihiro ABE
Michitaka SAKAIDA

Abstract

An imaging diagnosis apparatus for brick walls inside coking chambers of coke-oven batteries was developed and put into practical use. The huge wall with a high temperature exceeding 1 000°C was observed by a large-sized heat-resistant probe equipped with multiple line cameras and laser projectors. Irregularity measurement was performed in conjunction with thermal imaging. The data obtained by the apparatus is extremely useful for coke-oven batteries that have been in operation for many decades. Texture analysis, which recognizes a specific object on a given image, can be applied to the quantification of carbon adhesion on the wall. The increase of pushing load, which is a major problem for aging coking chambers, was clarified by modeling the irregular shape of the damaged portion on the wall.

1. Introduction

When the use period of coke oven batteries exceeds 30 years, decrease in the production capacity and energy efficiency due to deteriorated ovens begins to gradually arise. On the coking chamber wall composed of firebricks, various types of damage are observed. When irregularities on the chamber walls due to wear damage and partial defects become aggravated, in particular, the pushing load when extracting coke cake increases, which stops the pusher, causing production problems. As well as reconstructing deteriorated coke oven batteries, Nippon Steel Corporation has been actively developing maintenance technologies required to maintain the operation of aged coke oven batteries. Coking chamber diagnosis apparatuses[1, 2] that Nippon Steel developed have been playing an important role in coke oven diagnostic techniques. Such apparatuses photograph the entire walls of high-temperature, narrow coking chambers and measure their 3D profiles. This paper outlines the coking chamber diagnosis apparatus and introduces example usage of chamber wall image data and irregularity data that are obtained through diagnosis.

2. Coking Chamber Diagnosis Apparatus

If the temperature of a coke oven made of silica bricks is lowered once, thermal shock damages the bricks, which lowers the strength of the oven, so the inside is constantly maintained at a high temperature of approximately 1 000°C. Additionally, coal is heated from combustion chambers on both sides via the brick walls, and due to this structure, a coking chamber is 16 m long and 6 m high but only 0.4 m wide. Therefore, it is difficult to know if there is any uneven wall damage deep inside the chamber just by observation from the chamber door. In some diagnosis methods, heat-insulated small image sensors[3, 4] or apparatuses that measure oven width at a certain height[5, 6] are installed onto pushers and inserted into coking chambers. However, those apparatuses provide only partial observation of the walls. Nippon Steel has developed a diagnosis apparatus which enables the entire wall measurement with high accuracy. An outline is shown below.

2.1 Heat-resistance diagnosis probes

The coking chamber diagnosis apparatus consists of a platform moving on the rails of a pusher and a diagnosis probe to be inserted into a chamber. The diagnosis probe is inserted into the chamber from the door on the pusher side (hereinafter, PS). Electronic devices for measurement such as CCD cameras, lasers, and the like are mounted at the tip of the probe. Since the temperature inside the coking chamber is high, cooling water is circulated inside the probe exterior and cooling air is also supplied to the inside. This cooling mechanism maintains the inside of the probe equal to or lower than 40°C. Glass that shields infrared rays is used as the observation windows for the cameras and lasers to prevent temperature increase due to incidental thermal radiation. Diagnosis of walls is carried out in an empty coking chamber after discharging the coke by a pusher. The probe promptly goes forward and backward in the chamber within approximately four minutes so as to have as little impact on

* Senior Researcher, Ph.D., Instrumentation & Control Research Lab., Process Research Laboratories
20-1 Shintomi, Futtsu City, Chiba Pref. 293-8511

the coke production as possible.

Figure 1 (a) illustrates the horizontal section of the diagnosis probe. Line scan cameras, each of which is tipped with a linear image sensor as a photodetection element, are used to photograph thermal radiation from a high-temperature chamber wall. The linear viewing field of the camera is set along the vertical direction to the chamber wall and line brightness signals are obtained for each millimeter as the probe advances to form an image. The oven height of 6 m is covered by four cameras with 2048 pixels arranged in the vertical direction. A wall image having the resolution of 1 mm in the horizontal direction and 0.75 mm in the vertical direction is thus obtained. When the camera looks at the wall directly in the narrow chamber, the camera views the wall at an acute angle as shown by the broken line in Fig. 1 (a). Consequently, the unavoidable swaying of the probe in the width direction creates the problem of a deformed image resulting from the largely unstable viewing position. As a solution to this problem, a 6-m-high mirror manufactured from a stainless steel pipe with polished surfaces is set in front of the cameras. The mirror can bend the view direction so that the camera can perpendicularly observe the chamber wall and this function can decrease the influence of the displacement of the probe in the chamber width direction. The inside of the pipe is water-cooled in order to prevent high temperature oxidation of the metallic mirror surface. The camera mounted on a motor-driven stage rotates right and left and it obtains images of the right wall and the left wall on the way to and from the opposite side of the chamber.

The prime characteristic of the diagnosis apparatus is that it takes a thermal image of a chamber wall and at the same time measures irregularities on the wall by the laser light-section method in one-time observation of the inside of the chamber. Plural laser beams are projected from obliquely below or obliquely above in the field of view of the camera as shown in Fig. 1 (b). The laser beams are projected at intervals of 130 mm, nearly equal to the height of one brick. The probe is equipped with 44 small laser diodes, which are separately positioned in the upper section and in the lower section. When the probe proceeds while obtaining an image with projected laser light spots, the reflected intensities of the laser lights on the image are observed as lines in the horizontal direction. According to the principle of the light-section method, the laser line on an image is rectilinear if the wall is flat, but the laser line fluctuates vertically if an irregularity exists. The specifications, such as laser wavelength, intensity, and wavelength selection filter of the line camera, were determined such that the balance of the contrast of laser reflected light would be appropriate against the thermal radiation brightness of the chamber wall.

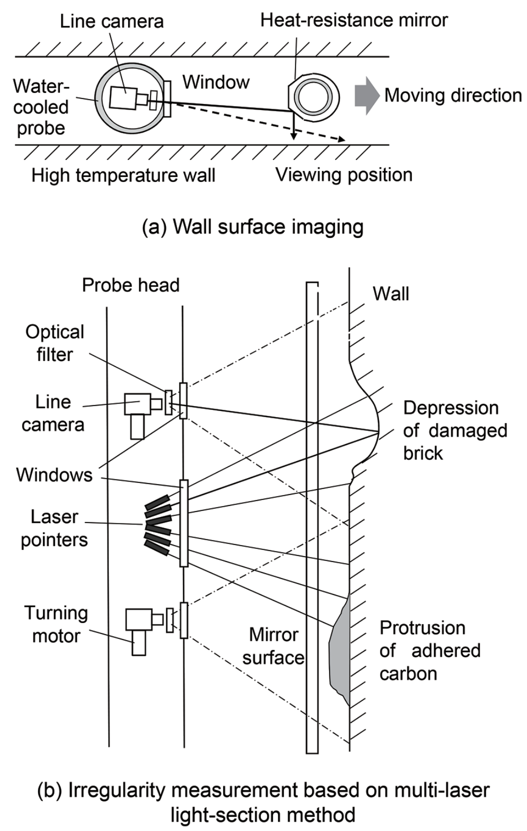

Fig. 1 Optical measurement system of heat-resistance diagnosis probe[1)]

Figure 2 shows an example of a portion of a chamber wall image. Carbon partially adheres to the chamber wall, in general. In the region of bare brick, the joints and vertical cracks are filled with carbon. The carbon region seems brighter than the surface of the bricks. This may be because the carbon is burning due to air from the door getting into the coking chamber during the diagnosis. At the sections where the laser beams are partly distorted, the wall is uneven.

2.2 Measurement software

In the measurement of irregularities on chamber walls, signal processing software is an important development item. To obtain the 3D profile of a chamber wall based on up-and-down displacement of multiple laser lines on an image, the laser lines are first tracked in the horizontal direction. A problem was to distinguish a horizontal joint line from the laser line accurately because their gray level on images is not clearly different. Image processing for detecting the laser line by focusing on the difference in the width of the two types of lines was derived.[7)] The relationship between laser line displacement on the image and the irregularity on the wall is determined based on the geometric conditions of the imaging system such as laser emission angle and image resolution. Two types of 3D profiles measured at intervals of 40 mm and 4 mm in the horizontal direction are created.

The inclination and meandering of the diagnosis probe need to be corrected to obtain accurate 3D irregularity data. Such correction is described below. **Figure 3** (a) shows an example of raw 3D profile data measured at intervals 40 mm. At first glance, there is a projection below position A in the longitudinal direction and a depression

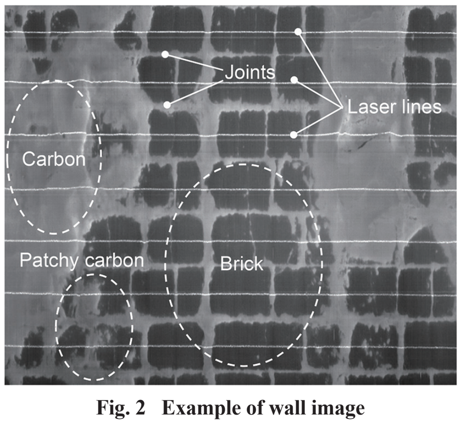

Fig. 2 Example of wall image

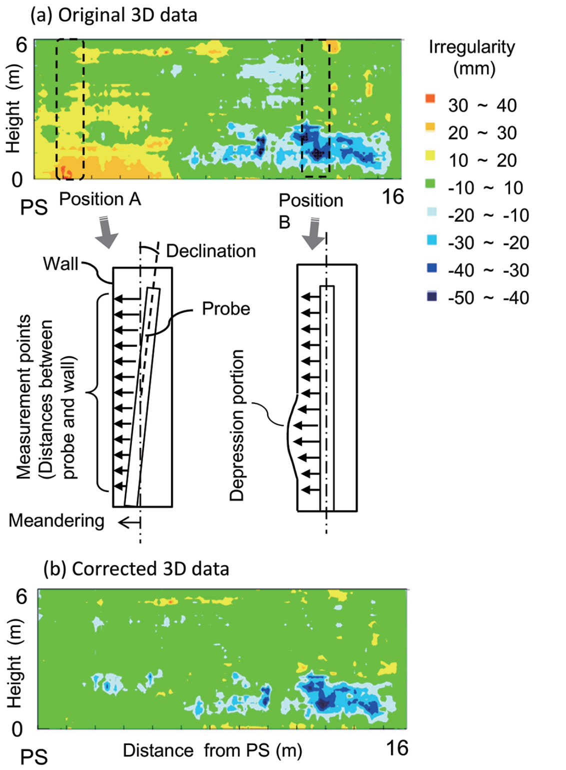

Fig. 3 Correction of pseudo irregularity on wall 3D profile data[8)]

near position B. However, when looking at it carefully, the projection amount linearly decreases in the height direction at position A. This indicates that the chamber wall has no irregularity; however, the lower part of the diagnosis probe tilts toward the chamber wall. Thus, it is not a true irregularity, but it is a pseudo irregularity due to the tilted probe. When the probe meanders, similar disturbance occurs in irregularity measurement. Therefore, we studied signal processing to extract the true volume of an irregularity on a chamber wall from the raw irregularity data including a mix of the inclination and meandering of the diagnosis probe.[7, 8)] The probe equipped with line cameras has rigidity and it remains straight, so a pseudo irregularity due to the inclination is seen on the entire wall. On the other hand, the top and bottom of chamber wall bricks are restrained, so deformation of the brick surface appears only at part of the wall. A straight line is fitted in the height direction of the irregularity data at positions in the longitudinal direction of a chamber wall and sections that deviate from this straight line were regarded as deformed chamber wall sections. Such signal processing can remove the probe inclination and meandering from raw data to obtain the true irregularity distribution as shown in Fig. 3 (b).

3. Chamber Wall Diagnosis based on Images

Figure 4 shows the images of the walls of coking chambers for which the years of operation are different. The images clearly show changes in the chamber walls over time. Once commercial coking chamber diagnosis apparatuses were introduced into some coke-making plants, many findings on damage to chamber walls were acquired from accumulated image data. For example, vertical cracks over multiple levels of bricks are observed at almost regular intervals on all of the coking chamber walls in operation for many decades. Presumably such vertical cracks were formed due to swelling and contraction of the bricks when normal-temperature coal was

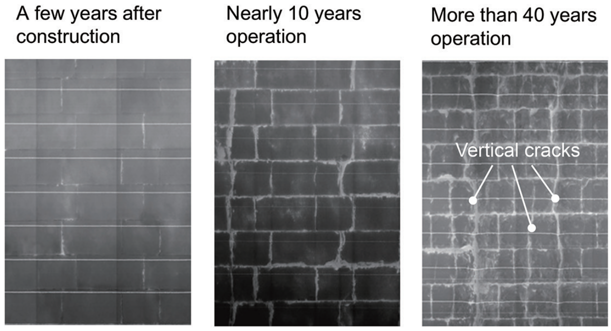

Fig. 4 Long-term changes of chamber-wall surfaces[8)]

charged and heated; then, such cracks gradually enlarged and the number and width thereof increased. The progress of cracks that affect the structural strength of chamber walls is considered to be a factor in determining the coke oven life.

Next, image processing that quantifies adhered carbon is described below as a case where chamber wall image data is used.[9)] A coke oven battery has approximately 100 coking chambers and the area and distribution of adhered carbon vary among them. Carbon is filled in depressions on walls to smooth them. However, excess growth becomes a protrusion. Therefore, on aged coking chambers, carbon adherence needs to be appropriately managed.

We classified the growth of carbon into the three states shown in the ovals with the broken lines in Fig. 2. The state where carbon has adhered only to the joints and cracks is referred to as “brick.” The state where carbon has completely covered the bricks is referred to as “carbon.” The state between “brick” and “carbon” where carbon has grown on joints and cracks greater than their width is referred to as “patchy carbon.”

Carbon is characteristically brighter than the surrounding brick surface. However, carbon on an entire chamber wall cannot be accurately identified by simple binarization alone. This is because chamber wall images are thermal imaging of high-temperature radiation and thereby the gray level of images varies depending on the temperature distribution on the chamber walls. Therefore, texture analysis that finds specific objects on an image based on gray-level distribution and patterns was applied for recognizing the carbon states.[9)]

In texture analysis, streaky patterns of joints and vertical cracks are targeted and preprocessing is performed to emphasize these streaks in the horizontal and vertical directions. Then, the image is divided into small-size blocks such that each includes a joint or crack without exception and the texture features listed below are calculated.

(1) Histogram features: In the case of carbon, the differences in the gray level in a block are small and the gray level histogram is close to being symmetrical. This appearance is quantified based on the skewness and variation coefficient of the histogram.

(2) Gray level co-occurrence matrix features: This method calculates the statistics on the gray-level of two certain pixels at relative positions in a block and captures the uniformity and shape of the patterns as features. In our study, four features of the gray level co-occurrence matrix, angular secondary moment, contrast, entropy, and correlation, are used.

(3) Features based on binary images: These features are distance and mean gray-level obtained as follows: A binary image in which streak carbon along joints and cracks is extracted is cre-

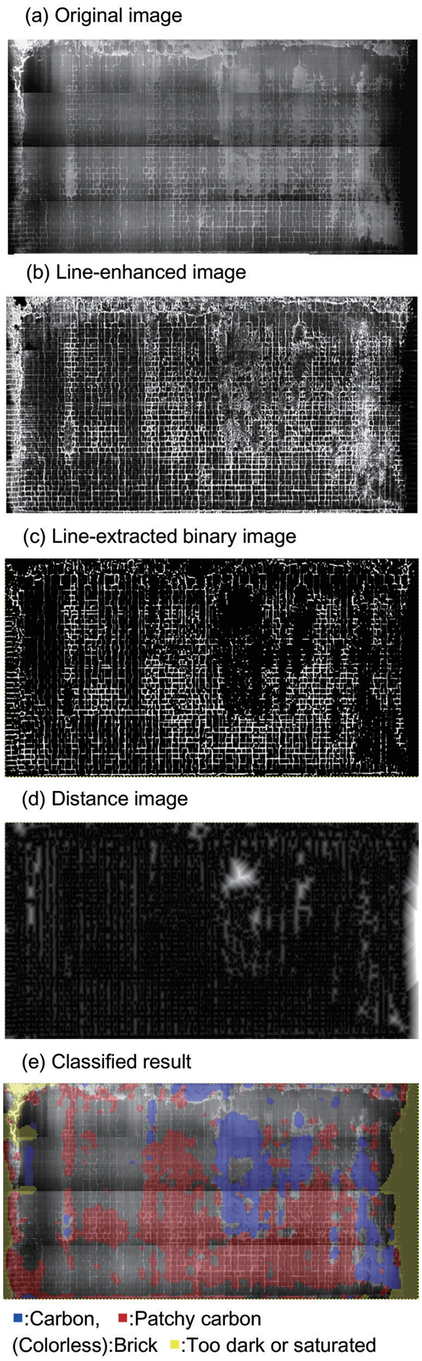

Fig. 5 Image processing for classification of wall carbon states [9]

ated; and intervals between bright regions in the vertical direction in a block and the mean brightness of the distance image (on which the distance from a target pixel to the nearest bright region is regarded as gray level) are obtained.

In the classification of chamber wall states based on these features, a support vector machine that is a popularized method as a machine learning technique was used. As training data, "bricks," "carbon," and "patchy carbon" from commercial coking-chamber wall images were visually selected and applied.

Figure 5 shows the image processing processes and an example of the wall surface classification result. Image (b) can be obtained from the original image (a) by preprocessing which emphasizes carbon streaks. This image was used to calculate the histogram features and gray level co-occurrence matrix features. Binary image (c) was obtained by extracting the carbon streaks in the horizontal and vertical directions at the regions composed of bare bricks. Distance image (d) was derived by further processing image (c). From images (c) and (d), the features based on the binary image were calculated. In the final image of the classification result (e), the three chamber wall states can be almost correctly distinguished except for both ends of the chamber wall where the image is too dark or saturated.

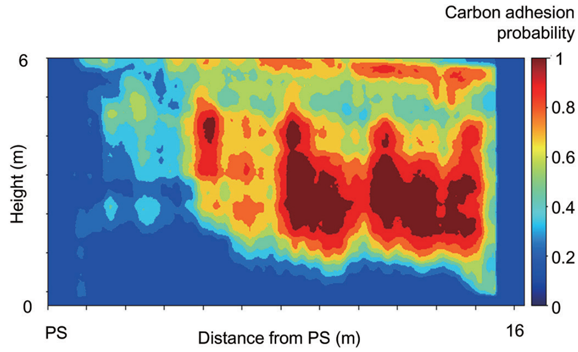

Fig. 6 Analysis of spatial distribution of carbon adhesion probability

For a single coke-making plant, carbon adherence patterns on many coking chambers were analyzed to study on which sections of chamber walls carbon tented to adhere. **Figure 6** shows the results. The width of the coking chamber gradually enlarges from the PS toward the push-out direction by several tens of millimeters to make it easier to discharge coke cake. The temperature on the discharge side is higher than that at the PS to systematize the coking time, so the carbon grows faster at the chamber wall on the discharge side. In addition, the figure shows that more carbon has adhered in the regions immediately below the five coal charging holes where the brick surface has roughened. In addition to these, air flow of a carbon incineration lance affects the carbon distribution. This type of analysis is used to explore desirable carbon distribution to prevent pushing loads from increasing.

4. Influence of Chamber-wall Irregularities on Pushing Loads

The pushing load of coke cake varies depending on a number of factors such as charge coal amount, contraction volume after coking based on coal blending and moisture content, and heating time. Irregularities on chamber walls directly and significantly affect the pushing loads. 3D profiles of chamber walls have revealed that there are many forms of irregularities: Some depressions are large but rather gentle while others are steep and deep. A single chamber wall sometimes has multiple depressions. A depression on a chamber wall is subjected to thermal spraying to flatten the surface in repair. However, such work takes a few hours to fill a single depression and the coke production is suspended during the repair. To secure coke output, pushing loads need to be effectively lowered in a limited repair time; however, at first, it could not be objectively determined which irregularities have to be preferentially repaired. Therefore, we developed a technique to estimate the increase in pushing loads based on the shape of irregularities on chamber walls.[1, 2, 10)]

4.1 Macroscopic irregularities on chamber walls

If a protrusion exists on a chamber wall, it is obvious that a moving coke cake has come into contact with the protrusion and thus receives resistance. Coke cake is not a consolidated solid but an aggregation of coke lumps divided by cracks that are formed during coking. There are interspaces, resulting from shrinkage during heating, among lumps and between the lumps and the wall. In order for the coke to pass over any protrusion on a chamber wall, it is surmised that the movement as well as the rotation of coke lumps occur expending the interspaces, before an insufficient space for this movement causes compacted lumps to crumble. It is difficult to express such a behavior with a physical model. Therefore, the present study addresses expression in the form of an experimental equation on the relationship between an irregularity on a chamber wall and the resistance received by moving coke cake.

Figure 7 illustrates the horizontal cross section inside a coking chamber with a depression on one side of the wall. The profile of the chamber wall can be expressed by discrete irregularity depth z at intervals of 40 mm. The differential between the adjoining z is defined as Δz. Δz is positive when the chamber width is narrowed in the push-out direction. Now, if the coke cake is pushed in the right direction in Fig. 7, the coke in the section n and $(n+1)$ comes into contact with the wall. It is assumed that resistance force is generated depending on the steepness and length of the wall's slope in contact with the coke cake.

We have defined the value as the partial resistive index which indicates the resistance at the time of pushing. The partial resistive index, k, is determined from Δz, as described in the following. In "Zone $(n-1)$" and "Zone $(n+2)$", the partial resistive index, k, is zero as the coke lumps are not in contact with the chamber wall. When Δz is less than fine gap δ corresponding with the interspace between the coke lumps and chamber wall, k is also zero. δ was determined as 2 mm as a value corresponding to shrinkage between the coke cake and oven wall. Assuming that the resistance in proportion to the power of Δz_n corresponding to the gradient of the wall is created in "Zone n," where the coke lumps are in contact with the wall slope, the partial resistive index, k_n, is given by Equation (1):

$$k_n = (\Delta z_n - \delta)^{\alpha} \qquad (1)$$

where, α is a constant. "Zone $(n+1)$" is a continuous slope climbing from anterior adjacent "Zone n." Since it is considered that the resistance force should be higher when gaps being δ or larger are continuous than when isolated gaps are scattered, the value obtained by multiplying the partial resistive index in the anterior zone by constant β is added to Equation (1) in such a zone. Specifically, the partial resistive index, k_{n+1}, in "Zone $(n+1)$" is presented by the following Equation (2):

$$k_{n+1} = (\Delta z_{n+1} - \delta)^{\alpha} + \beta \times k_n \qquad (2)$$

Although only one side of the chamber wall has a depression in Fig, 7, the resistance against the pushed coke cake should be dictated by the displacement in the chamber width. Therefore, the partial resistive index is calculated from the total of the Δz values in the opposing position when the chamber wall has irregularities on both sides.

Next, the partial resistive index is weighted according to the height of the chamber wall. This is because coke cake requires larger force to pass an irregularity in the inferior part of the wall to one in the upper section even when the shape of the irregularities is the same since the lower the coke cake is situated in the coking chamber, the more undeformable it is due to the constraint of self-weight. Such a condition is formularized as in the following. The partial resistive index, k'_n, at the height of h from the chamber floor is expressed by the following Equation (3):

$$k'_n = \left\{1 + \frac{\gamma(H_0 - h)}{H_0}\right\} \times k_n \qquad (3)$$

where, H_0 is the height from the chamber floor to the ceiling and γ is the weighing constant according to the height position.

The partial resistive indices are calculated at intervals of 40 mm in the horizontal direction at approximately 40 positions to which the laser beams are projected. The total value over the full coverage of the chamber wall is referred to as the resistive index. Parameters α, β, and γ in Equations (1) to (3) are empirically determined so that the calculated resistive index that shows the irregularity state of the coking chamber can be linearly associated with the pushing load. A laboratory setup simulating a portion of a coking chamber was assembled for pushing load measurement at room temperature. The measured parameter α was 1.45, β was 0.2, and γ was 1.

Figure 8 shows an example of a 3D profile of one portion cut out from a coking chamber wall including relatively large depressions. The lateral axis denotes the distance from the pusher side and the vertical axis denotes the height from the floor of the coking chamber. The depression occurring at the worn brick surface has a depth of 50 mm at the deepest point. The projections are adhered carbon. **Figure 9** shows the spatial distribution of the partial resistive indices calculated in respect to the shape of the wall in Fig. 8. On the slope toward the push-out direction from the bottom of the

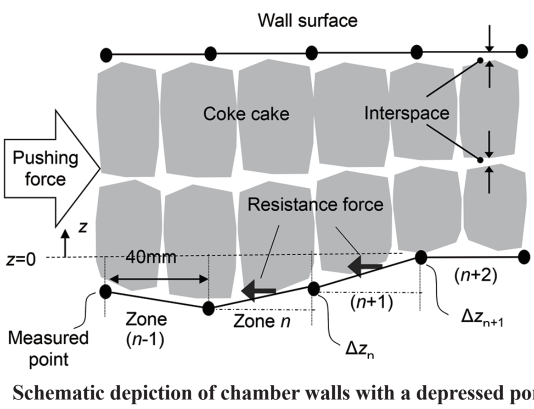

Fig. 7 Schematic depiction of chamber walls with a depressed portion[1]

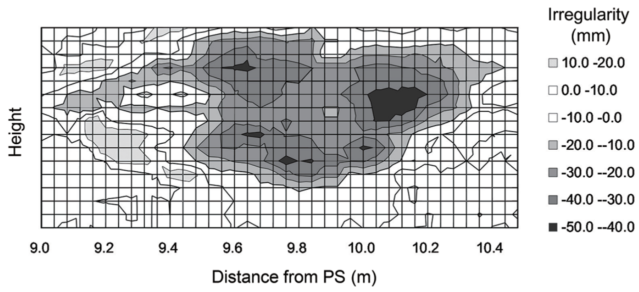

Fig. 8 Example of chamber-wall terrain[2]

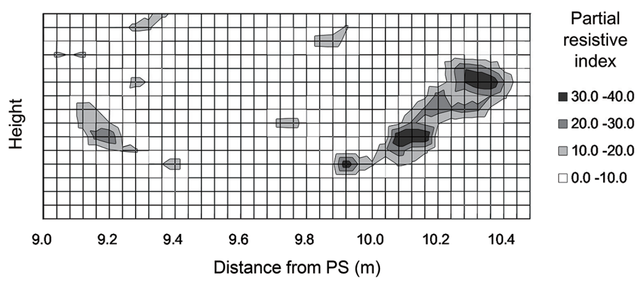

Fig. 9 Spatial distribution of partial resistive indices[2]

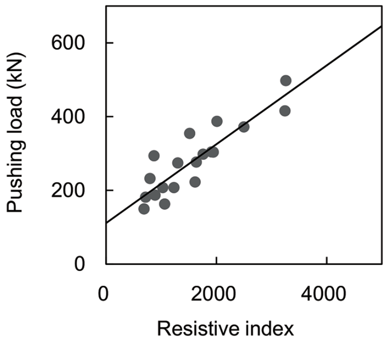

Fig. 10 Relationship between resistive index and pushing load[2)]

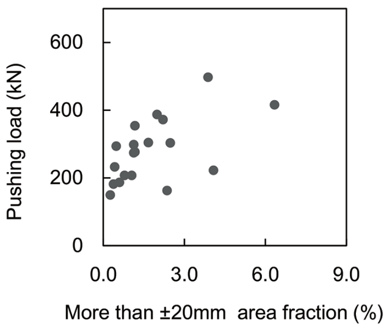

Fig. 11 Relationship between uneven area and pushing load[2)]

large depression, partial resistive indices are concentratedly observed.

Figure 10 shows the relationship between the resistive index and the pushing load with regard to coking chambers in which irregularities (damage) and adhered carbon vary. For comparison, regarding the same coke ovens, the relationship between the pushing load and the ratio of the uneven region with an irregularity of ±20 mm or more to the overall area of the wall is indicated in **Fig. 11**. Whereas the correlation between the resistive index and the pushing load as shown in Fig. 10 can evidently be confirmed, the relationship between the uneven area and the pushing load shown in Fig. 11 has poor correlation. This fact suggests that only focusing on the mere size of damaged areas does not allow us to correctly assess the harmfulness of the damage due to irregularities. The line in Fig. 10 denotes an approximation linear expression of the relationship between the resistive index and pushing load with an ordinate intercept of 111 kN and a gradient of 0.107. The relational expression having the intercept never falling to zero is consistent with the fact that a certain pushing load arises from the friction on the chamber wall and the floor even if the chamber wall is completely smooth. The resistive index that focuses on the shape and positions of regions of which coke comes into contact with irregularities on chamber walls has indicated the pushing load generation mechanism more appropriately.

The resistive index of the depression on the chamber wall in Fig. 8 is 940. Based on the previously described relational expression in Fig. 10, it is equivalent to approximately 100 kN of pushing resistance. By means of the estimation using the resistive index, we can gauge the increase in the pushing load posed by an irregularity. When a chamber wall has plural irregularities, the effects of thermal spraying for flattening the walls and the priority of repair can be quantitatively evaluated.

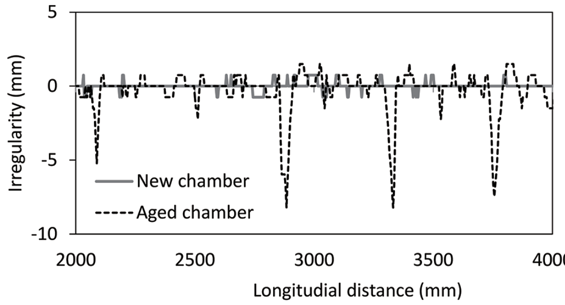

Fig. 12 Comparison of horizontal profiles between new and aged chamber walls

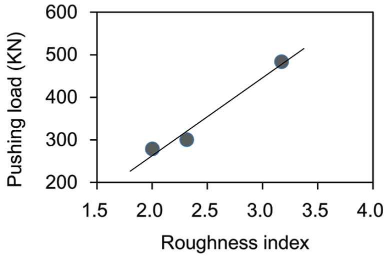

Fig. 13 Relationship between roughness index and pushing load[10)]

4.2 Microscopic irregularities on chamber walls due to vertical cracks

The resistive index targets phenomena in which coke cake comes into contact with conical depressions on chamber walls or projections arising from excessively developed carbon, which deteriorates the pushing. Another type of damage on aged coking chamber walls is the edge defects of bricks along vertical cracks. Such vertical cracks are observed on entire chamber walls, so we call such damage roughness of chamber walls. Increase in the pushing load due to the roughness of a chamber wall can be considered as a friction between the chamber wall and coke cake. If carbon that grows on chamber walls fills such minute depressions favorably, the frictional resistance can be lowered. Patchy carbon described in Chapter 3 may work well to smooth the wall roughness.

To observe the shape of rough sections, profile data of a chamber wall measured at intervals of 4 mm in the longitudinal direction is used. **Figure 12** shows examples of wall profiles in the chamber length direction. For the aged coking chamber, V-shaped grooves having a depth of several millimeters are observed at the vertical crack positions. To quantify the degree of such roughness (damage), the “roughness index” is used. The index is defined as follows: The maximum depth on the wall at intervals of 100 mm is extracted against the 4-mm pitch profile and the depth values are averaged for the entire chamber wall. **Figure 13** shows the relationship between the roughness index and pushing load for coking chambers with low resistive indices. Both the resistive index and roughness index should be managed as separate pushing load factors.

5. Conclusion

This paper described the special optical measuring apparatus for coking chamber wall inspection, along with the usage of diagnosis data. Nippon Steel has developed the apparatus that takes thermal images of a huge coking chamber wall while measuring 3D profiles by the laser light-section method. The apparatus has overcome the difficulties of high-temperature exceeding 1000°C and narrow width inside coking chambers and was put to practical use. After the utilization of such diagnosis apparatuses began at steelworks, many findings on the wall damage of aged coking chambers were obtained. Then study on diagnosis technologies, which can quantify the appearance of the chamber walls, advanced.

The coke-making process tends to rely on the experience of factory workers and engineers. Automatic recognition of adhered carbon distribution and clarification of the influence of wall irregularities on the pushing loads serve as an aid to understand the coke-making process scientifically, contributing to the stable production and longer life of oven batteries. In addition, the utilization of the chamber wall deterioration mechanism until such time that coke ovens exceed their life spans, which were found by analyzing diagnosis results, and quantitative data of dominant factors of chamber wall deterioration obtained from diagnosis results have enabled accurate estimation of service life. Nippon Steel has been replacing aged coke oven batteries systematically based on the estimated life prediction.

References

1) Sugiura, M. et al.: Trans. Soc. Instrum. Control Eng. 47 (10), 435 (2011)
2) Sugiura, M. et al.: ISIJ International. 53 (4), 583 (2013)
3) Hamaki, M. et al.: CAMP-ISIJ. 5, 1122 (1992)
4) Sugiura, M. et al.: CAMP-ISIJ. 17, 179 (2004)
5) Grosse-Wilde, M. et al.: Cokemaking Int. 8 (2), 42 (1996)
6) Sugiura, M. et al.: CAMP-ISIJ. 16, 296 (2003)
7) Sugiura, M. et al.: Proceedings of Asian Steel Conference 2015, 2015, p. 662
8) Sugiura, M.: Bull. Iron Steel Inst. Jpn. 23 (6), 257 (2018)
9) Sugiura, M. et al.: Proceedings of the SICE Annual Conference 2017, 2017, p.429
10) Sugiura, M. et al.: CAMP-ISIJ. 27, 796 (2014)


Masato SUGIURA
Senior Researcher, Ph.D.
Instrumentation & Control Research Lab.
Process Research Laboratories
20-1 Shintomi, Futtsu City, Chiba Pref. 293-8511


Yoshihiro ABE
Senior Researcher, Doctor of engineering
Instrumentation & Control Research Lab.
Process Research Laboratories


Michitaka SAKAIDA
General Manager, (Coke making Plant Engineering)
Plant Engineering Div.
Plant Engineering and Facility Management Center